Microsyst Technol (2016) 22:2499–2509
DOI 10.1007/s00542-015-2638-9

TECHNICAL PAPER

High-speed and precision control of a piezoelectric positioner with hysteresis, resonance and disturbance compensation

Geng Wang[1] · Guoqiang Chen[1] · Fuzhong Bai[2]

Received: 11 May 2015 / Accepted: 22 July 2015 / Published online: 6 August 2015

Abstract A novel composite control strategy is developed in this paper to compensate hysteresis, resonance and disturbances in a piezo-actuated nanopositioner. The control objective of the piezoelectric positioner is to achieve high tracking performance in terms of accuracy and speed. For this purpose, a Bouc–Wen model based hysteresis compensator is first applied to mitigate the hysteresis nonlinearity without the complex inverse hysteresis calculation. And then, the linear dynamic of the hysteresis compensated system is identified and inverted to account for the resonance. A model-based inversion feed-forward controller is designed to achieve high speed tracking. Afterwards, a high-gain feedback controller is designed based on a notch filter to handle the modeling inaccuracy and all kinds of disturbances. So, the feed-forward controller can be augmented to the feedback controller to realize high speed and precision tracking. The enhancement of tracking performance is demonstrated through several comparative experiments. The performance of 70 Hz bandwidth and 0.281 μm precision can be achieved, which validated the effectiveness of the proposed composite control scheme.

1 Introduction

Nanoscientific research and related nanotechnology have developed rapidly in the last three decades. One of the key requirements of nanotechnology is nanopositioning, which is essential for a range of applications including data storage (Vettiger et al. 2002), scanning and microscopic technology (Tuma et al. 2012; Braunsmann and Schaffer 2010), piezo-actuated flexure stages (Chae et al. 2011), optical deflectors (Wang et al. 2014), resonant scanners (Humphris et al. 2005), fast steering mirrors (Wang and Rao 2015; Wang et al. 2015), deformable mirrors (Ruppel et al. 2011) and MEMS microscanners (Pantazi et al. 2007). Among the diverse drive methods, nanopositioning using piezoelectric actuation is one of most common methods for nanometre-scale, because piezoelectric actuator has low inertia, fast response, sub-nanometre resolution, high bandwidth and large force generation (Higuchi 2010). However, precise nanopositioning using piezoelectric actuation over a broad range of frequencies has still been a challenge.

In many nanoscientific studies and applications, high-precision positioning, high tracking bandwidth and robustness to different operating conditions are simultaneously required. As for piezoactuated nanopositioning system, the main obstacles when achieving the above objective come from nonlinear effects of piezoelectric material such as hysteresis and creep that limit the positioning accuracy, from resonant modes that limit the bandwidth, and from disturbance issues that can affect the robustness to modeling uncertainties and operating conditions. Many efforts have been made in the literature to deal with the above problems.

Hysteresis nonlinear effect of piezoelectric material is one of the main factors which affect the accuracy of nanopositioning system. In low frequencies, the positioning error produced by the hysteresis nonlinearity can be up to 15 % of the total moving range (Ge and Jouaneh 1996). Beyond the first resonant frequency, oscillation or instability will even occur. To alleviate the hysteresis, many

✉ Geng Wang
wgmouse@163.com

[1] School of Mechanical and Power Engineering, Henan Polytechnic University, Jiaozuo 454003, China

[2] College of Mechanical Engineering, Inner Mongolia University of Technology, Huhhot 010051, China

modeling and compensation methods have been proposed in the literature. For example, the Prandtl–Ishlinskii model (Al Janaideh et al. 2011), the Bouc–Wen model (Rakotondrabe 2011), the Preisach model (Viswamurthy and Ganguli 2007), frequency domain characterization (Gozen and Ozdoganlar 2012), the Maxwell's slip model (Goldfarb and Celanovic 1997), hysteron model (Tao and Kokotovic 1995) are utilized to characterize the hysteresis behavior and their inverse models are used to linearize the actuator response. However, the inverse models are usually difficult to obtain and the direct model should be as accurate as possible which limits the further improvements in positioning accuracy. On the other hand, the approaches which do not require hysteresis model are also proposed, which treat the unmodeled hysteresis as a disturbance (Chang et al. 2009). For instance, the sliding mode control (Fuqing et al. 2014), neural network control (Liaw and Shirinzadeh 2009), H-infinite robust control (Chen et al. 1999), fuzzy control (Lin and Li 2014) have been reported in the literatures. Yet, only tackling the hysteresis nonlinearity is not enough because the resonant dynamics of nanopositioning system can restrict the further improvement of the control accuracy over a broad range of frequencies.

The resonant modes of nanopositioning system is another big challenge which must be tackled to achieve high bandwidth control and thus obtain a high positioning accuracy in the high speed motions. Due to the resonant modes, the effective operating frequency of closed-loop system is restricted to less than 1/10–1/100th of the first resonance frequency of the nanopositioning system (Clayton et al. 2009). Although the piezoelectric positioner can be made to be sufficiently stiff and small, the traversal range is limited to a few microns. To eliminate the effects of resonant dynamics, many efforts have been made by the researchers to deal with this problem. From the point of view of automation, development of control methods is a more popular and effective way. In the literature, several approaches have been developed to damp the resonant dynamics, such as, the notch filters (Gu and Zhu 2013), integral resonant controllers (Gu et al. 2014), input shaping controllers (Vorbringer-Dorozhovets et al. 2011), inversion-based controllers (Liu 2014), positive position feedback control (Mahmood and Moheimani 2009) and so on. It should be noted that before these control strategies are developed, the hysteresis nonlinearity should be sufficiently eliminated in advance.

The robustness to noise and disturbances is also a big problem which is related to the performance of nanopositioning system. To address this problem, the use of feedback control is inevitable. Many modern or intelligent controllers have been investigated, such as the robust H-infinite controller (Wu and Zou 2009), adaptive-based controller (Shieh and Hsu 2008), learning-based controller (Huang et al. 2014), high-gain PD (proportional plus differential) controller (Leang and Devasia 2007) and so on. However, these feedback controllers have little success in tracking waveforms whose high-frequency harmonics are outside of the bandwidth of the closed-loop system. As a result, the positioning accuracy often becomes lower at higher speeds.

As can be seen from above, various control methods have been investigated to mitigate the hysteresis, resonance and disturbance. To achieve nanopositioning at high speed and high precision simultaneously, development of control techniques where hysteresis, resonance and disturbance are all well considered is a promising way. Unfortunately, this kind of comprehensive control method is still scare up to now. Ref. Croft et al. (2001) developed an integrated controller where the hysteresis was linearized by the inverse Preisach model, the resonance was suppressed by using the inversion of vibrational dynamics and the disturbances were alleviated by feedback loop. Lei Liu et al. (2013) presented a composite control method and realized high-speed and precision scanning where the inverse Preisach model and inverse dynamics are used to mitigate the hysteresis and vibrations, and a proportional-integral (PI) controller is used to suppress the unknown disturbances. Guo-Ying Gu et al. (2013) presented a work where an inverse of the Prandtl–Ishlinskii model was used to cancel the hysteresis effect and a notch filter was adopted to compensate for the vibration and a feedback controller is utilized to account for the noise and disturbances. Yet, the inverse hysteresis models in the above methods are all difficult to solve due to the complex computations. Different from the existing methods, in this paper a Bouc–Wen model based control approach is proposed to account for these three factors. This is a novel composite control strategy, whose enhanced performance is demonstrated in terms of speed and accuracy though comparative experimental results.

The purpose of this paper is to demonstrate the design and the effectiveness of the proposed composite method, by which the high-speed and precision positioning of piezoelectric actuator can be achieved. The main features of this method lie on that: (1) the inversion based feedforward technique is used to realize high bandwidth, and a high-gain feedback controller is utilized to further improve the control performance; (2) a Bouc–Wen hysteresis model is directly used in the feedforward controller, which does not need complex computation for developing an inverse hysteresis model; (3) the linear dynamics is identified and its inverse is derived to be employed in the feedforward controller; (4) a notch filter is designed to enable the use of the high-gain feedback controller which can handle the modeling inaccuracy and all kinds of disturbances. Moreover, the proposed control strategy is simple and easy to implement in practice. Experimental results confirmed the effectiveness of the proposed method.

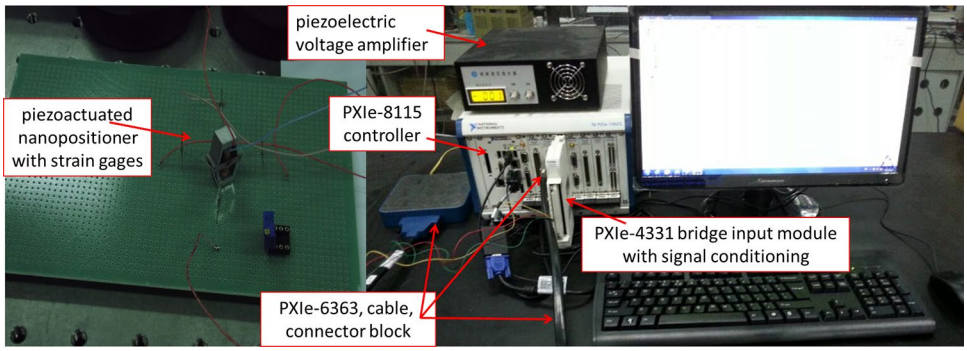

Fig. 1 Experiment setup

The remainder of this paper is organized as follows. Section 2 details the experimental setup. Section 3 presents the design of a composite controller which is used to realize high-speed and precision tracking. In this section, the hysteresis nonlinearity and resonant dynamics are identified and inverted to be used as a feedforward controller, and a high gain feedback controller is designed to handle the disturbances. In Sect. 4, several comparative experiments are conducted to verify the effectiveness of the proposed composite controller. And conclusions are drawn in Sect. 5.

2 Experimental setup

The experimental setup is shown in Fig. 1, which consists of a miniature piezoelectric positioner, a strain gage sensor, a real-time controller and a voltage amplifier. In the experiment, the displacement output of piezoelectric positioner is measured with accuracy of 80 nm by the strain gages glued on its mechanical framework. The output signal of strain bridge is acquired, amplified and filtered by a dynamic bridge input module (PXIe-4331, NI Corp.) with 24-bit resolution A/D converters. The PXIe-8115 Platform (NI Corp.) equipped with LabVIEW software was used to implement the real-time control procedure for the piezoelectric positioner. And the control signal was outputted by a NI X Series Multifunction DAQ device (PXIe-6363) with 16-bit resolution D/A converters, and then amplified by a piezoelectric voltage amplifier (from IOE, CAS) before applying to piezoelectric positioner. The sampling rate of the control loop is set to 20 kHz.

3 Controller design

One of the important control objectives in high-speed nanopositioning is to minimize the difference between the desired trajectory and the actual trajectory over broadband frequencies. For this purpose, a comprehensive control scheme shown in Fig. 2 is first proposed in this paper to realize the high-speed and high-precision tracking control

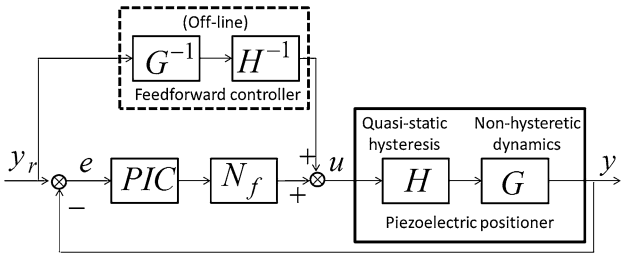

Fig. 2 Block diagram of control scheme

for the piezoelectric positioner. An inversion based feedforward controller is employed to realize high control bandwidth where H^{-1} represents inverse quasi-static hysteresis and G^{-1} is the inverse dynamics. In the feedback loop, a high-gain PI type feedback controller (PIC) is employed to mitigate the disturbances and the modeling errors within feedback bandwidth. The notch filter N_f is utilized here to damp the first resonant mode and thus enable the use of a high-gain feedback controller. It should be noted that the parameters in feedforward controller are obtained by offline identification with PSO algorithm and frequency response method. In the following, the development of this composite control scheme will be presented in detail.

Remark 1: As we know, there are many studies that utilize a combination of hysteresis model, feedforward, and feedback compensation. However, the objective of this work is focusing on the improvement of tracking speed and precision. Ref. Gu and Zhu (2013) realized the compensation of creep, hysteresis and vibration, but the inverse of linear dynamics is not used which restricts the speed. The feedback linearization of piezoactuator in AFM is also performed in Ref. Leang and Devasia (2007), however the hysteresis part is not modeled which restricts the precision.

Remark 2: To the best of our knowledge, the Bouc–Wen model is seldom used in the high bandwidth control scheme. Usually, the P-I model is used instead, such as Gu and Zhu (2013), Gu et al. (2014). In fact, the inverse of Bouc–Wen model is more simple and easier to be implemented. This improves the performance of the proposed control scheme.

3.1 Identification and compensation of quasi-static hysteresis of piezoelectric positioner

As we know, the dynamic behavior of piezoelectric positioner can be characterized by rate-dependent hysteresis (Gu and Zhu 2011), which can be effectively decomposed into the cascade connection of quasi-static hysteresis and non-hysteretic dynamics (Wong et al. 2012; Gu et al. 2013). In this paper, the piezoelectric positioner is modeled by a linear two order dynamic model cascaded with a Bouc–Wen hysteresis model. And in this subsection, the identification and compensation of the Bouc–Wen hysteresis model will be briefly discussed in advance.

3.1.1 Bouc–Wen hysteresis model and its identification

The Bouc–Wen model was first proposed by Bouc in 1967 and later extended by Wen in 1976. Mathematically, it is simple and only has very fewer parameters. By choosing appropriate parameters, it is often used to describe a wide variety of hysteresis with various shapes. In the literatures, for example (Zhenyan et al. 2012), the Bouc–Wen model has been verified to be able to describe the hysteresis phenomenon in the piezoelectric positioner. The input–output relationship described by Bouc–Wen model can be established by the following nonlinear differential Eq. (1):

$$\begin{cases} y = dV - h \\ \dot{h} = \alpha \dot{V} - \beta \left|\dot{V}\right| h - \gamma \dot{V} |h| \end{cases} \tag{1}$$

where y denotes the displacement output, V is the input voltage, d is a parameter representing the piezoelectric coefficient, h is a nonlinear hysteretic term. The shape of hysteretic loop is determined by the three coefficients α, β and γ.

Generally, the parameters of Bouc–Wen model can be identified through different methods such as the adaptive estimation approach or evolutionary algorithms. In this work, the particle swarm optimisation (PSO) algorithm which is a kind of evolutionary algorithm is used to identify the three parameters of the Bouc–Wen model, because this method is with great performance and easy to be implemented (Chen and Li 2007). The key point of this method is to select the fitness function which is used to verify the model performance. In order to accurately fit the data between model outputs and experimental results, the fitness function is selected as:

$$f(\alpha, \beta, \gamma, d) = \sqrt{\sum_{i=1}^{L} (Y_{\text{exp}}^i - Y_{BW}^i)^2 / \sum_{i=1}^{L} (Y_{\text{exp}}^i)^2} \tag{2}$$

where, Y_{exp}^i denotes the output data from the experiment at the ith sampling time, Y_{BW}^i is the output data from Bouc–Wen model, and L is the total number of samples. In the experiments the discrete-time form of Bouc–Wen model (1) is used, therefore the parameter optimization problem can be described as follows:

$$\begin{aligned} &\min \quad f(\alpha, \beta, \gamma, d) \\ &\textit{subject to} \quad \begin{cases} y_k = dV_k - h_k \\ h_k = h_{k-1} + \Delta t(\alpha \dot{V}_k - \beta \left|\dot{V}_k\right| h_{k-1} - \gamma \dot{V}_k |h_{k-1}|) \end{cases} \end{aligned} \tag{3}$$

where, Δt is the discrete time interval.

With the experimental setup in Sect. 2, the parameters in Bouc–Wen model (1) is identified based on the PSO methods. As the model is static, the frequency of excitation signal should be low enough to avoid exciting the response of dynamics and not too low to avoid the creep effect. During the experiment, the frequency of excitation signal is selected as 1 Hz through trial method. With the modeling error of 2 %, we obtained the identified parameters $\alpha = 0.78[\mu\text{m/V}]$, $\beta = 0.009[\text{V}^{-1}]$, $\gamma = 0.007[\text{V}^{-1}]$, $d = 2.0[\mu\text{m/V}]$. Figure 3 shows the comparison between experimental hysteretic loop and simulated Bouc–Wen hysteretic model. We can see that the simulated model output can distinctly reach the experimental hysteretic output to achieve an excellent fitting result.

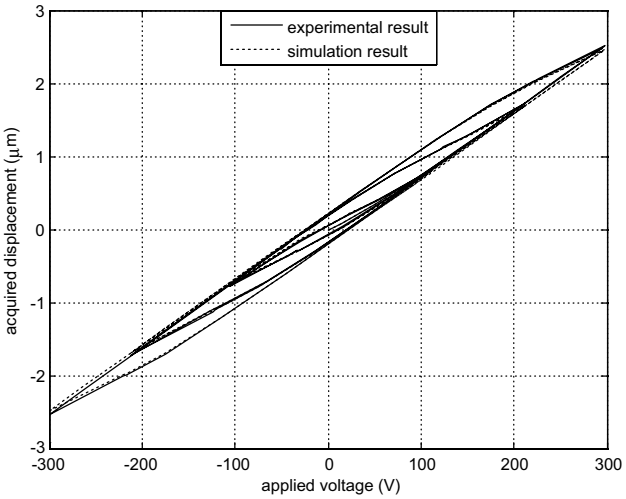

Fig. 3 Hysteresis identification results

3.1.2 Direct inversion compensation based on Bouc–Wen model

In this subsection, the Bouc–Wen model is used to compensate the quasi-static hysteresis based on a direct inversion method (Rakotondrabe 2011), where this model can be directly used for hysteresis compensation without modeling the hysteresis inverse. The merits lie in the effectiveness of computation and the easiness of implementation.

From the control point of view, a compensator H^{-1} must be designed so that the displacement output of Bouc–Wen

model can reach the reference input of the compensator. Considering the direct hysteresis model (1), the hysteresis compensator H^{-1} can be designed as:

$$\begin{cases} V = (y_r + h)/d \\ \dot{h} = \alpha\dot{V} - \beta|\dot{V}|h - \gamma\dot{V}|h| \end{cases} \tag{4}$$

where, V is the output of compensator, y_r is the reference input of compensator.

It can be seen that the compensator is an inverse operation of the direct model (1) and does not required any inversion of hysteresis. Moreover, no additional computation is required because the parameters α, β, γ and d are already known during the process of modeling and identification. The hysteresis compensation scheme is shown in Fig. 4. It should be noted that the hysteresis compensator is only used to compensate the quasi-static hysteresis because the above Bouc–Wen model (1) is static and rate independent.

In the following, the hysteresis compensator H^{-1} is used to linearize the piezoelectric positioner. A 1-Hz sinusoidal reference signal is passed though the hysteresis compensator H^{-1} and then utilized to drive the piezoelectric positioner. The correctness and effectiveness of the hysteresis compensator H^{-1} is validated by the experimental results shown in Fig. 5. It can be seen that the Bouc–Wen model based feedforward compensator can be used to eliminate nonlinear hysteresis to some extent. The positioning error with Bouc–Wen compensator is much smaller than the one without Bouc–Wen compensator.

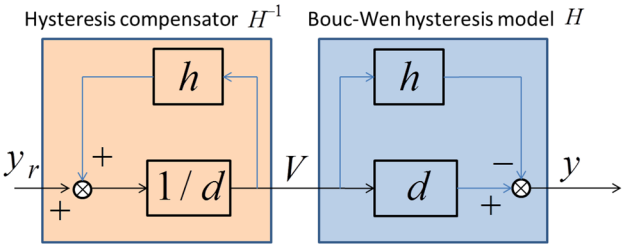

Fig. 4 Direct inversion hysteresis compensation scheme

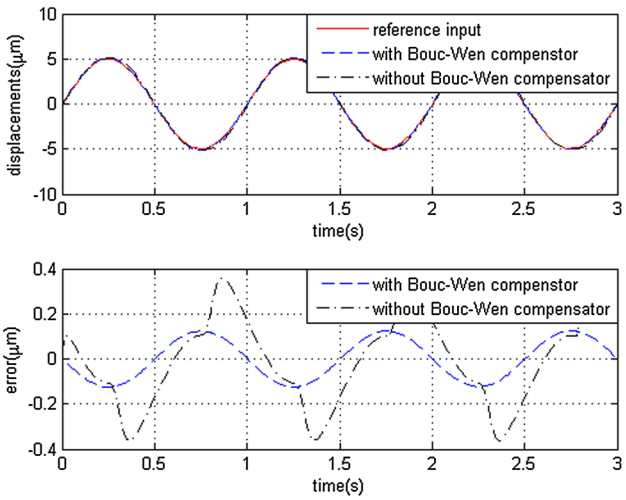

Fig. 5 Bouc–Wen feedforward compensation

3.2 Identification and compensation of nonhysteretic dynamics

3.2.1 Identification of the linear dynamics

As mentioned before, a reasonable model of piezoelectric positioner can usually be regarded as a linear non-hysteretic dynamic model preceded by a nonlinear quasi-static hysteresis component (Wong et al. 2012; Gu et al. 2013). In Sect. 3.1, the hysteresis part has been compensated in advance. In this section, the frequency response experiment is conducted to investigate the non-hysteretic linear dynamics of the hysteresis compensated system. For this purpose, a small-amplitude band-limited white noise signal is used to excite the piezoelectric positioner with hysteresis compensation. The test results of the frequency response are shown in Fig. 6, which reveals the first resonant mode occurs around 95 Hz. A linear second-order dynamic model was obtained by the Levy method, and can be expressed by

$$G = \frac{3.62 \times 10^5}{s^2 + 35.6s + 3.62 \times 10^5} \tag{5}$$

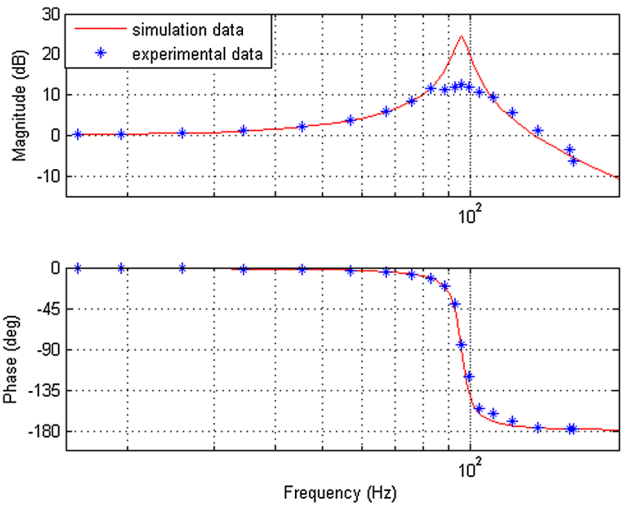

Fig. 6 Frequency response of the piezoelectric positioner

It can be seen that the identified second-order model matches the system dynamics well in the frequencies bellow 100 Hz.

Remark 3: It is worth mentioning that the excitation signals should have a relatively high frequency to capture the dynamic response when the creep effect can be conservatively neglected. And it should also be noticed that the influence of hysteresis effect on dynamical identification results can also be omitted because the hysteresis has been compensated in advance.

3.2.2 *Feedforward compensation based on model inverse approach*

In this subsection, a feedforward approach (Garrett et al. 2009; Kam et al. 2009) is employed to simultaneously account for the hysteresis and dynamics of the piezoelectric positioner so as to achieve a high bandwidth tracking control. The feedforward approach shown in Fig. 7 is based on the inverse model and can be used to compensate the phase-lag and magnitude distortion, which encompasses the inverse non-hysteretic dynamics and the inverse static hysteresis. Initially, a desired signal is passed through the inverse non-hysteretic dynamics $\hat{G}^{-1}$ and then through the inverse static hysteresis $\hat{H}^{-1}$ to generate the feedforward control input u_{ff}. In subsection 3.1.2, the details of the inverse static hysteresis $\hat{H}^{-1}$ have been given. And now, the inverse non-hysteretic dynamics $\hat{G}^{-1}$ is derived. Considering the expression (5), the inverse non-hysteretic dynamics $\hat{G}^{-1}$ can be given in the following.

$$\hat{G}^{-1} = \frac{s^2 + 35.6s + 3.62 \times 10^5}{3.62 \times 10^5} \tag{6}$$

It should be noted that the transfer function in Eq. (6) has more zeros than poles and thus cannot be directly implemented. To solve this problem, s^2 and s can be respectively replaced with $\frac{s^2}{\varepsilon s^2+1}$ and $\frac{s}{\varepsilon s+1}$ where ε is a small positive value. When the desired reference signal is known and sufficiently smooth, the derivative $dr(t)/dt$ can be used to replace s. Thus, the inverse non-hysteretic dynamics $\hat{G}^{-1}$ can be represented in time domain. Then, the model-based inversion feed-forward controller u_{ff} can be expressed in the following:

$$u_{ff} = y_r \cdot (\hat{G}^{-1} \cdot \hat{H}^{-1}) \tag{7}$$

Based on the above approach, a feedforward control experiment is implemented with a known 40 Hz sinusoidal reference signal to validate the correctness and effectiveness of the feedforward controller. The experimental results are shown in Fig. 8. It can be observed that the reference signal can be well followed by the actual output with the inverse-based approach.

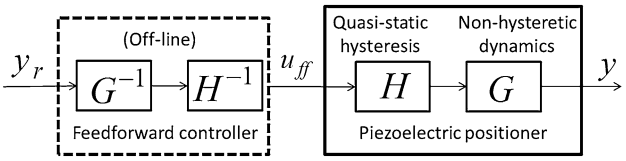

Fig. 7 The feedforward control approach

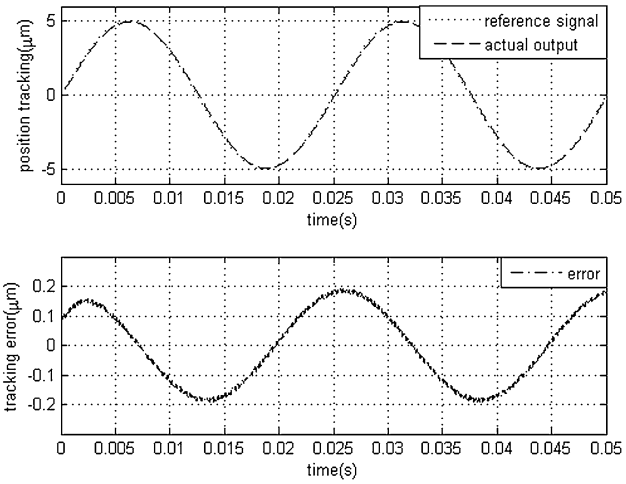

Fig. 8 The feedforward tracking control

3.3 Feedback controller design

Although the inversion based feedforward controller is suitable to achieve high speed performance, the use of feedback controller is inevitable which can guarantee the stability and robustness of system in the presence of disturbances and modeling errors. However, the feedback control can often result in low gain margin and potentially cause instability. Especially in the first resonant frequency, the gain of feedback control is severely limited. In this paper, a notch filter is used to cancel the effect of the resonant peak and raise the gain margin. And then a high-gain PI type feedback controller can be employed.

3.3.1 *Notch filter for vibration compensation*

The notch filter is a filter with a narrow stopband which makes it effective for eliminating the sharp resonance peak in the frequency response (Ando et al. 2008; Vorbringer-Dorozhovets et al. 2011). In this subsection, a notch filter is designed and employed to improve the tracking performance over the bandwidth of interest for the high-gain feedback controllers. A general structure of the second-order notch filter N_f is as follows:

$$N_f = k \cdot \frac{s^2 + 4\pi\zeta_n f_n s + 4\pi^2 f_n^2}{s^2 + 4\pi\zeta_d f_d s + 4\pi^2 f_d^2} \tag{8}$$

where k is the notch filter gain, ζ_d is the desired damp ratio, f_d is the desired natural frequency, ζ_n is the damp ratio of the controlled pant, f_n is the natural frequency of the controlled pant. In general, the values of ζ_n and f_n are selected according to the dynamics characteristics of the controlled pant. In this paper, ζ_n and f_n are respectively set to be 0.03 and 95.76 from the identified model (5). And in order to suppress the resonance of model (6), ζ_d and f_d are chosen to be 0.39 and 135 respectively. And then the frequency response of model (5) with notch filter (8) can be expressed as $N_f \cdot G$. The comparison of the frequency responses with and without notch filters is shown in Fig. 9, which reveals the sharp resonant peak has been completely damped. Therefore, the high bandwidth control can be achieved because the maximum bandwidth of closed-loop control system is inversely proportional to the magnitude of the lowest frequency resonance peak.

Remark 4: From Fig. 9, we can see that the gain margin is increased due to the introduction of notch filter. So, it is helpful to realize high speed tracking control.

3.3.2 Notch filter based high-gain feedback controller

As we know, the gains of feedback controller are limited by the low gain margin imposed by the resonance peak. In subsection 3.3.1, a notch filter is introduced and employed to increase the gain margin. This enables the use of high-gain feedback controller with higher control gains.

Among the various feedback controllers, such as, sliding model control, robust adaptive control, fuzzy control and proportional-integral-derivative control, the most popular choice is the proportional integral controller (PI) which is simple to implement and robust to modeling errors. Without loss of generality, the PI controller is designed with the following transfer function of the controller $C(s)$.

$$C(s) = k_p + \frac{k_i}{s} \tag{9}$$

where, k_p and k_i are the proportional gain and integral gain respectively, and the s is the Laplace operator. Generally, higher control gains mean faster trajectory convergence. However, the control gains must be set to trade off the stability and performance. In this paper, the feedback control gains (k_p and k_i) are manually tuned in the experiment and are chosen to be $k_p = 0.73$ and $k_i = 280$. Compared with the system without notch filter, the gain k_i increased from 20 to 280. Figure 10 shows the phase margin of the open-loop system increased from 4°(without filter) to 39°(with filter). And from Fig. 11 we can see that the corresponding −3 dB bandwidth of the closed loop system increased from 2.3 Hz (without filter) to 72 Hz (with filter). It indicates that the high tracking bandwidth of the system could be achieved with the high gain feedback controller.

4 Experimental results and discussions

Based on the proposed composite control scheme shown in Fig. 3, several experimental studies have been carried out with the piezoelectric positioning system present in Sect. 2. The superiority of the proposed controller in terms of accuracy and speed is verified by trajectory tracking experiments compared with different PI controllers.

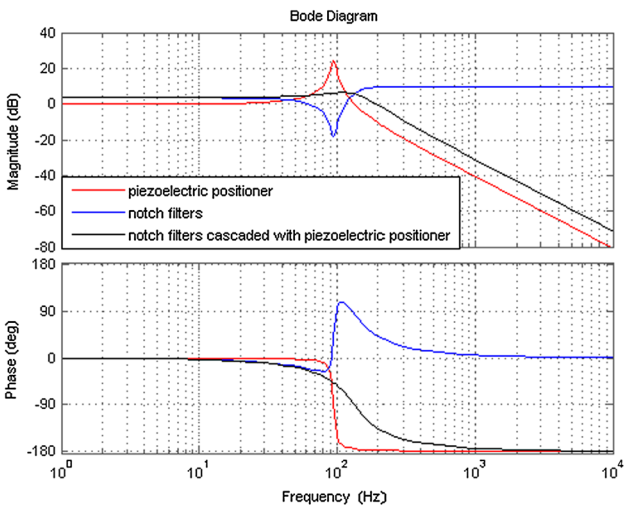

Fig. 9 Frequency response comparison of the system with and without filter

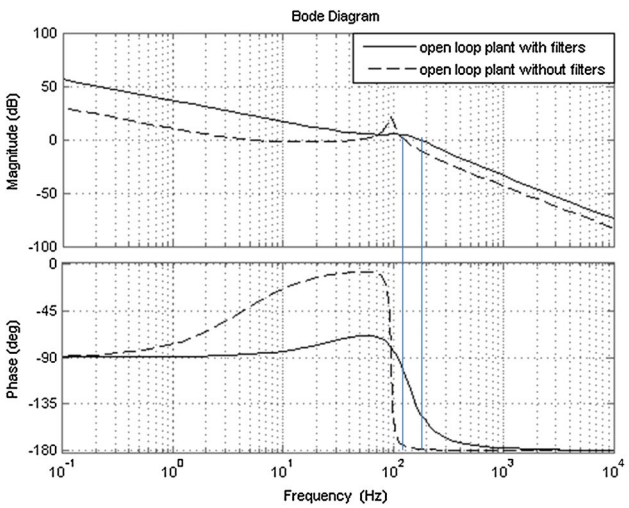

Fig. 10 Frequency response of open-loop system with and without filter

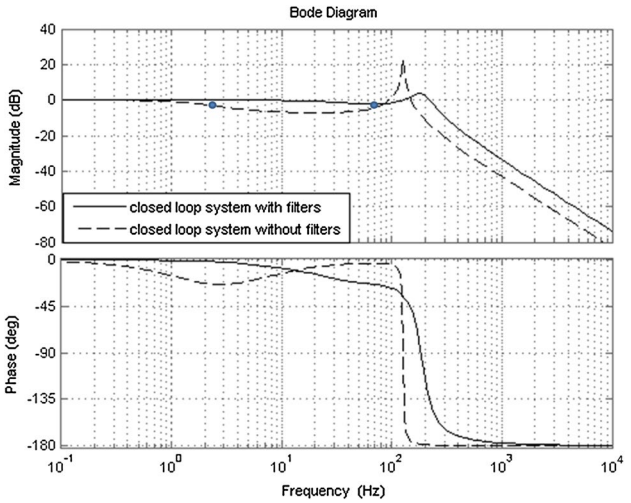

Fig. 11 Frequency response of closed-loop system with and without filter

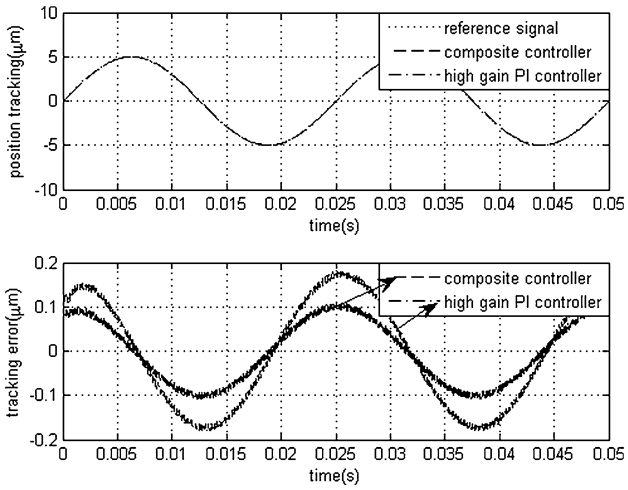

Fig. 12 Comparison of single frequency trajectory tracking

4.1 Performance indexes

In order to quantitatively evaluate the performance of the proposed controller, the following indexes are defined in advance.

1. $error(k) = x(k) - x_d(k)$: the definition of error.
2. $e_{pv} = \max(error(k)) - \min(error(k))$: the peak-to-valley value of error.
3. $e_{rms} = \sqrt{\frac{1}{n}\sum_{k=1}^{n} error(k)^2}$: the root-mean-square value of error.

4.2 Validation for high precision performance

The precision performance of the proposed composite controller is compared with the high gain PI controller through different trajectory tracking experiments.

First, a sinusoidal reference signal of 40 Hz is used for single frequency trajectory tracking, and the results are shown in Fig. 12 and Table 1. The tracking errors of e_{pv} and e_{rms} for the high gain PI controller are respectively 0.435 and 0.141 μm. Compared with the composite controller, the errors of e_{pv} and e_{rms} reduced to 0.173 and 0.046 μm, respectively. We can observe that the performance of the proposed composite controller is superior to the high gain PI controller in the tracking accuracy. This is further evidenced in the experiment for tracking multi-frequency reference signal $\sin(2\pi * 10 * t) + \sin(2\pi * 20 * t) + \sin(2\pi * 30 * t) + \sin(2\pi * 40 * t) + \sin(2\pi * 50 * t)$, and the experimental results are shown in Fig. 13 and Table 1. Obviously, the tracking errors of the composite controller are smaller than the high gain PI controller. That is, the proposed composite controller can achieve more precision performance according to the obtained experimental results.

Table 1 Comparison of tracking performances of different controllers

Performance indexes	High gain PI controller	Composite controller
Single- frequency		
e_{pv}	0.361	0.216
e_{rms}	0.116	0.068
Multi- frequency		
e_{pv}	0.386	0.225
e_{rms}	0.078	0.045

4.3 Validation for high speed performance

The high speed performance of the proposed composite controller, compared with a traditional PI controller, is verified in this subsection. Different reference signals (20, 50, 70 Hz) are used for trajectory tracking in the comparative experiments. The results are shown in Fig. 14 and Table 2. We can observe that the tracking errors increase gradually as the frequency increases. Meanwhile, the proposed composite controller can achieve better performance than the traditional PI controller at the same frequency. Moreover, the errors of composite controller are in the acceptable range when tracking reference signal of 70 Hz. However, the errors of traditional PI controller are too big to track reference signals of more than 50 Hz. From the obtained performance, we can conclude that the proposed composite controller is superior to the traditional PI controller in terms of speed and accuracy.

Remark 5: From the results of Sects. 4.2 and 4.3, it can be seen that the indexes of accuracy and speed can simultaneously be satisfied, which validates the superiority of the proposed controller. High speed and precision control of piezoelectric actuator needs to mitigate the hysteresis, vibration and disturbance. However, till now effective

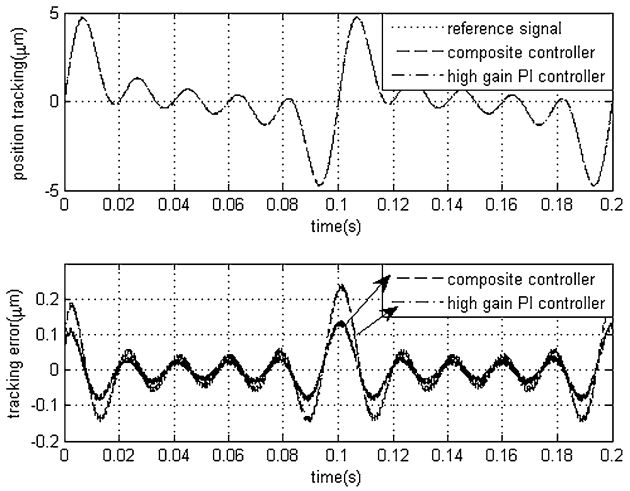

Fig. 13 Comparison of multi- frequency trajectory tracking

composite control strategies for simultaneously suppressing these three effects are still scarce, especially in the situation where Bouc–Wen model is utilized to describe and compensate the hysteresis. Compared with Gu and Zhu (2013) and Leang and Devasia (2007), the proposed control strategy is not only simple and easy to implement in practice, but also reaches excellent tracking performance.

5 Conclusions

This paper proposed a composite control strategy of piezo-actuated nanopositioner to realize high speed and precision tracking. This is a novelty and comprehensive control approach where hysteresis, resonance and disturbance are all well considered. As compared to the previous works, the main features of this paper are summarized as follows:

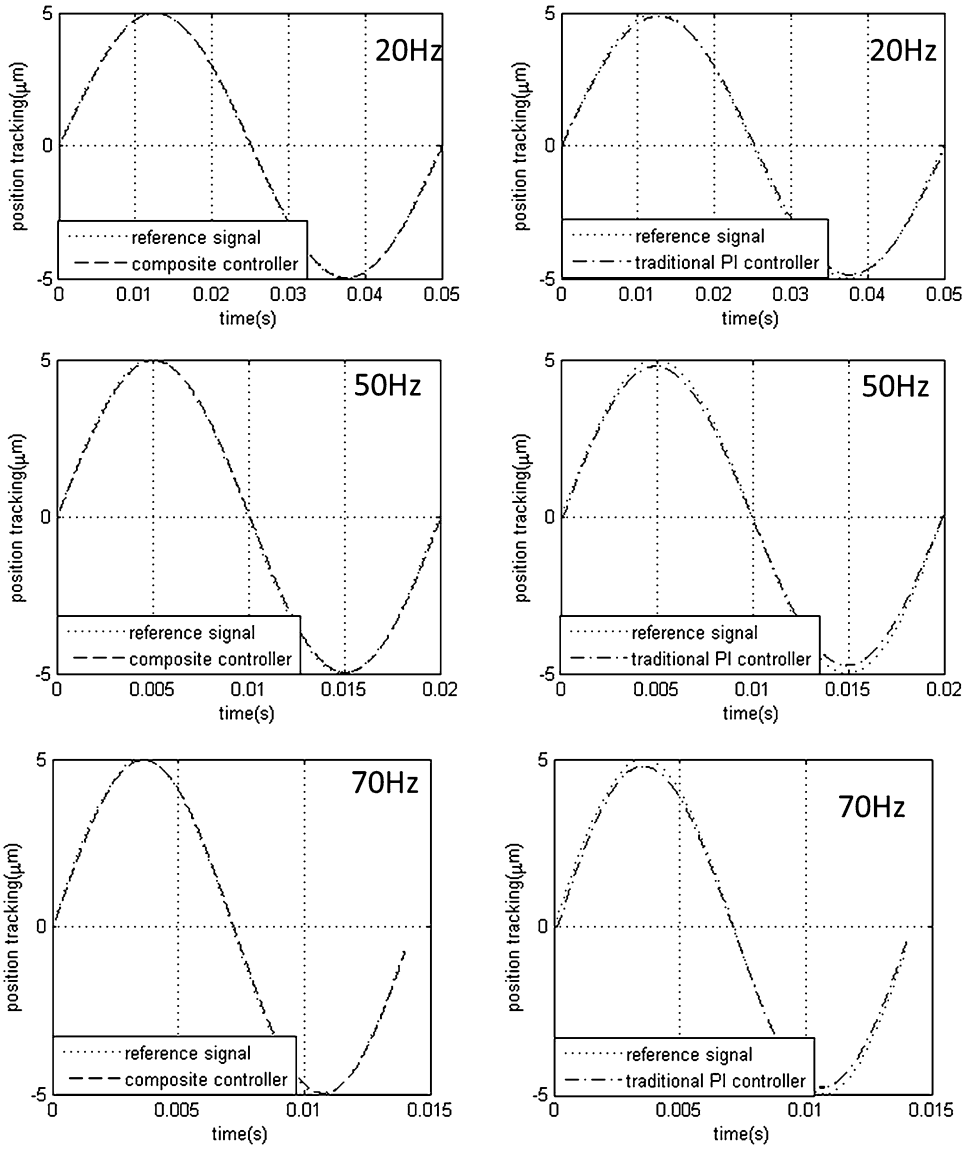

Fig. 14 Tracking experiments comparison for signals of different frequencies

Table 2 Comparison of tracking performances of different controllers

Performance indexes	PI controller	Composite controller
20 Hz		
e_{pv}	0.409	0.205
e_{rms}	0.137	0.064
50 Hz		
e_{pv}	0.513	0.267
e_{rms}	0.190	0.083
70 Hz		
e_{pv}	0.593	0.281
e_{rms}	0.189	0.088

1. A direct Bouc–Wen hysteresis model is designed to compensate for the hysteresis nonlinearity, which does not need complex computation for developing an inverse hysteresis model.
2. A model-based inversion control method is used to achieve high speed tracking.
3. A notch filter and a high-gain feedback controller are employed to handle the disturbances and modeling uncertainty.
4. Finally, a series of comparative experiments are performed to verify the effectiveness of the proposed composite control approach.

Acknowledgments This work was supported by the Doctoral Science Foundation of Henan Polytechnic University under Grant No. 60407/010.

References

Al Janaideh M, Rakheja S, Su CY (2011) An analytical generalized Prandtl–Ishlinskii model inversion for hysteresis compensation in micropositioning control. IEEE/ASME Trans Mechatron 16(4):734–744

Ando T, Uchihashi T, Fukuma T (2008) High-speed atomic force microscopy for nanovisualization of dynamic biomolecular processes. Prog Surf Sci 83:337–437

Braunsmann C, Schaffer TE (2010) High-speed atomic force microscopy for large scan sizes using small cantilevers. Nanotechnology 21:225705

Chae KW, Kim W-B, Jeong YH (2011) A transparent polymeric flexure-hinge nanopositioner, actuated by a piezoelectric stack actuator. Nanotechnology 22:335501

Chang S, Yi J, Shen Y (2009) Disturbance observer-based hysteresis compensation for piezoelectric actuators. In: Proceedings of American control conference, pp 4196–4201

Chen X, Li Y (2007) A modified PSO structure resulting in high exploration ability with convergence guaranteed. IEEE Trans Cybern 37(5):1271–1289

Chen BM, Lee TH, Hang CC, Guo Y, Weerasmriya S (1999) An H-infinite almost disturbance decoupling robust controller design for a piezoelectric bimorph actuator with hysteresis. IEEE Tran Autom Control 7(2):160–174

Clayton GM, Tien S, Leang KK, Zou Q, Devasia S (2009) A review of feedforward control approaches in nanopositioning for high-speed SPM. J Dyn Syst Meas Control 131(6):061101

Croft D, Shed G, Devasia S (2001) Creep, hysteresis, and vibration compensation for piezoactuators: atomic force microscopy application. ASME J Dyn Syst Meas Control 123(1):35–43

Garrett MC, Szuchi T, Kam KL et al (2009) A review of feedforward control approaches in nanopositioning for high-speed SPM. J Dyn Syst Meas Control-Trans ASME 131(6):061101

Ge P, Jouaneh M (1996) Tracking control of a piezoceramic actuator. IEEE Trans Control Syst Technol 4(3):209–216

Goldfarb M, Celanovic N (1997) Modeling piezoelectric stack actuators for control of micromanipulation. IEEE Contr Syst Mag 17(3):69–79

Gozen BA, Ozdoganlar OB (2012) A method for open-loop control of dynamic motions of piezo-stack actuators. Sens Actuators A Phys 184:160–172

Gu GY, Zhu LM (2011) Modeling of rate-dependent hysteresis in piezoelectric actuators using a family of ellipses. Sens Actuators A Phys 165(2):202–209

Gu G, Zhu L (2013a) Motion control of piezoceramic actuators with creep, hysteresis and vibration compensation. Sens Actuat A Phys 197:76–87

Gu G-Y, Zhu L-M (2013b) Motion control of piezoceramic actuators with creep, hysteresis and vibration compensation. Sens Actuators A Phys 197:76–87

Gu GY, Zhu LM, Su CY, Ding H (2013) Motion control of piezoelectric positioning stages: modeling, controller design and experimental evaluation. IEEE/ASME Trans Mechatron 18(5):1459–1471

Gu G, Zhu L, Su C (2014) Integral resonant damping for high-bandwidth control of piezoceramic stack actuators with asymmetric hysteresis nonlinearity. Mechatronics 24(4):367–375

Higuchi T (2010) Next generation actuators leading breakthroughs. J Mech Sci Technol 24:13–18

Huang D, Xu J-X, Venkataramanan V, The Cat Tuong Huynh (2014) High-performance tracking of piezoelectric positioning stage using current-cycle iterative learning control with gain scheduling. IEEE Trans Industr Electron 61(2):1085

Humphris ADL, Miles MJ, Hobbs JK (2005) A mechanical microscope: high-speed atomic force microscopy. Appl Phys Lett 86:034106

Leang KK, Devasia S (2007) Feedback-Linearized inverse feedforward for creep, hysteresis, and vibration compensation in AFM piezoactuators. IEEE Transac Control Syst Technol 15(5):927–935

Leang KK, Zou Q, Devasia S (2009) Feedforward control of piezoactuators in atomic force microscope systems inversion-based compensation for dynamics and hysteresis. IEEE Control Syst Mag 29(1):70–82

Liaw HC, Shirinzadeh B (2009) Neural network motion tracking control of piezo-actuated flexure-based mechanisms for micro-/nanomanipulation. IEEE/ASME Trans Mechatron 15(4):517–527

Lei L et al (2013) Discrete composite control of piezoelectric actuators for high-speed and precision scanning. IEEE Trans Ind Inf 9(2):859–868

Lin C-M, Li H-Y (2014) Intelligent control using the wavelet fuzzy CMAC backstepping control system for two-axis linear piezoelectric ceramic motor drive systems. IEEE Trans Fuzzy Syst 22(4):791–802

Liu L, Tan KK, Lee TH (2014) Multirate-based composite controller design of piezoelectric actuators for high-bandwidth and precision tracking. IEEE Trans Control Syst Technol 22:2

Mahmood I, Moheimani S (2009) Making a commercial atomic force microscope more accurate and faster using positive position feedback control. Rev Sci Instrum 80:063705

Pantazi A, Sebastian A, Cherubini G, Lantz M, Pozidis H, Rothuizen H, Eleftheriou E (2007) Control of MEMS-based scanning-probe data-storage devices. IEEE Trans Control Syst Technol 15:824–841

Rakotondrabe M (2011) Bouc–Wen modeling and inverse multiplicative structure to compensate hysteresis nonlinearity in piezoelectric actuators. IEEE Trans Autom Sci Eng 8(2):428–431

Ruppel T, Osten W, Sawodny O (2011) Model-based feedforward control of large deformable mirrorsg. Eur J Control 3:261–272

Shieh HJ, Hsu CH (2008) An adaptive approximator-based backstepping control approach for piezoactuator-driven stages. IEEE Trans Ind Electron 55(4):1729–1738

Tao G, Kokotovic PV (1995) Adaptive Control of Plants with Unknown Hysteresis. IEEE Trans Autom Control 40(2):200–212

Tian F, Li K, Wang J, Wang H (2014) Adaptive backstepping sliding mode control of fast steering mirror driven by piezoelectric actuator. High Power Laser Part Beams 26(1):59–63

Tuma T, Lygeros J, Kartik V, Sebastian A, Pantazi A (2012) High-speed multiresolution scanning probe microscopy based on Lissajous scan trajectories. Nanotechnology 23:185501

Vettiger P, Cross G, Despont M et al (2002) The millipede-nanotechnology entering data storage. IEEE Trans Nanotechnol 1:39–55

Viswamurthy S, Ganguli R (2007) Modeling and compensation of piezoceramic actuator hysteresis for helicopter vibration control. Sens Actuators A Phys 135(2):801–810

Vorbringer-Dorozhovets N, Hausotte T, Manske E, Shen JC, Jager G (2011) Novel control scheme for a high-speed meteorological scanning probe microscope. Meas Sci Technol 22(9):094012

Wang G, Rao C (2015) Adaptive control of piezoelectric fast steering mirror for high precision tracking application. Smart Mater Struct 24(3):035019

Wang G, Guan C, Zhang X, Zhou H, Rao C (2014) Precision control of piezo-actuated optical deflector with nonlinearity correction based on hysteresis model. Opt Laser Technol 57:26–31

Geng W, Jianwei N, Fuzhong B (2015) High precision tracking control of piezoelectric fast steering mirror based on self-tuning PID algorithm. J Henan Polytech Univ (Natural Science) accept

Wong PK, Xu Q, Vong CM, Wong HC (2012) Rate-dependent hysteresis modeling and control of a piezostage using online support vector machine and relevance vector machine. IEEE Trans Ind Electron 59(4):1988–2001

Wu Y, Zou Q (2009) Robust inversion-based 2-DOF control design for output tracking: piezoelectric-actuator example. IEEE Trans Control Syst Technol 17(5):1069–1082

Zhenyan W, Zhen Z, Jianqin M (2012) Precision tracking control of piezoelectric actuator based on Bouc–Wen hysteresis compensator. Electron Lett 48(23):1459–1460